Journal of Medical and Health Studies
ISSN: 2710-1452
DOI: 10.32996/jmhs
Journal Homepage: www.al-kindipublisher.com/index.php/jmhs

JMHS
AL-KINDI CENTER FOR RESEARCH AND DEVELOPMENT

| RESEARCH ARTICLE

Development and validation of CT-based radiomics to predict the nuclear grade of clear cell renal cell carcinoma

Jingwei Zhao[1], Yike Zhao[1]✉ and Lei Xu[1]✉
[1]Department of Radiology, Beijing Anzhen Hospital, Capital Medical University, Beijing, China
Corresponding Author: Yike Zhao and Lei Xu, **E-mail**: anzhenzyk@163.com; Email: Lei Xu: anzhenxl@163.com

| ABSTRACT
To construct a CT-based radiomics model to preoperatively predict the Fuhrman grade of clear cell renal cell carcinoma(ccRCC).173 ccRCC patients from The Cancer Imaging Archive(TCIA) were enrolled in this study. Radiomics features were derived from preoperative CT images of patients with ccRCC. The radiomics signature (Rad-score) was constructed using the least absolute shrinkage and selection operator algorithm. The Rad-score's predictive performance was assessed using the receiver operating characteristic (ROC) curve. Calibration curves were generated to evaluate the radiomics model's calibration. Eight features were selected to construct the Rad-score. The area under the ROC of the Rad-score was 0.800 in the training cohort and 0.710 in the validation cohort. There was high consistency confirmed by the Hosmer-Lemeshow test between the actual and predicted probabilities in the training(p=0.218) and validation (0.067) cohort. Our CT-based radiomics model can preoperatively predict Fuhrman grade in ccRCC patients.

| KEYWORDS
radiomics, clear cell renal cell carcinoma, Fuhrman grade, CT

| ARTICLE INFORMATION
ACCEPTED: 02 August 2025 **PUBLISHED:** 26 September 2025 **DOI:** 10.32996/jmhs.2025.6.4.13

Introduction

Renal cell carcinoma (RCC) is the most prevalent malignant tumor affecting the kidney [1]. Among its diverse pathological subtypes, clear cell renal cell carcinoma (ccRCC) stands out as the most common [2]. Nuclear grade is an important factor influencing the prognosis of clear cell carcinoma patients[3]. A previous study reported that individuals categorized as Fuhrman grade III or IV had a risk of metastasis four times greater than those with grades I or II[4]. Therefore, nuclear grade is crucial for patients in selecting appropriate treatment methods.

The Fuhrman grading system, which takes into account factors such as nuclear size, nuclear shape, and nucleolar prominence, is a widely adopted pathological grading system used to classify RCC[5]. Percutaneous biopsy is a method used for preoperative pathological grading assessment in RCC. However, it falls short in terms of accuracy, with an accuracy rate of only 43% when compared to postoperative specimens, which serve as the gold standard for diagnosing pathological grading [6]. Another study similarly reported that the accuracy of diagnosing Fuhrman grade through percutaneous core biopsy is 46%[7]. In addition to the problem of unsatisfactory accuracy, percutaneous biopsy can also potentially lead to some complications, with the most common being hematoma[8]. Therefore, developing a non-invasive and accurate method for preoperatively assessing the Fuhrman grading of RCC patients is highly necessary. Such advancements would not only enhance diagnostic precision but also mitigate the risks and inconveniences associated with invasive procedures, ultimately facilitating more informed and effective treatment decisions for patients with renal cell carcinoma.

Radiomics is an innovative field in medical imaging that involves the quantitative analysis of various features extracted from medical images[9]. This approach has the potential to capture and quantify the heterogeneity of tumors, providing valuable insights into their characteristics. The application of radiomics has the potential to address a multitude of clinical challenges, offering the possibility of resolving various clinical issues in healthcare. Radiomics has seen some applications in RCC. Previous research efforts have not only focused on distinguishing ccRCC from non-clear cell renal cell carcinomas using preoperative CT images[10], but they have also leveraged these images to predict the risk of recurrence in RCC[11]. Furthermore, radiomics has been employed in prior studies to anticipate the effectiveness of immunotherapy in RCC[12], highlighting the versatile potential of radiomics in addressing a range of clinical issues.

The aim of this study is to utilize CT-based radiomics to preoperatively predict the Fuhrman grade of ccRCC.

Methods

Patient selection

We downloaded the data of the patients involved in this study from The Cancer Imaging Archive (TCIA), a publicly available database[13]. The collection (TCGA-KIRC) we used contains 237 ccRCC patients with preoperative CT images. The clinicopathologic factors, including age, sex, laterality, Fuhrman grade, and pathological TNM stage of the patients involved in this study, were downloaded from the TCIA. Patients with Fuhrman grade I and II are classified into the low-grade group, while those with Fuhrman grade III and IV are categorized into the high-grade group. Patients in this study were included based on the following criteria. Inclusion criteria: (1) pathologically confirmed ccRCC. (2) with preoperative venous phase CT images. Exclusion criteria: (1) Lack of clinical information mentioned above. (2) patients receiving neoadjuvant treatment. (3) patients with multiple lesions. Since all data involved in this study are anonymous and publicly available, the approval of the institutional review board was exempt. Patients from two centers(TCGA-BP and TCGA-CJ) were assigned to the training cohort. Patients from the rest centers(TCGA-B0, TCGA-B8, TCGA-CW, TCGA-CZ, TCGA-DV, and TCGA-G6) were assigned to the external validation cohort. The data analyzed in this retrospective study were obtained from TCIA. TCIA belong to public databases. The patients involved in the databases have obtained ethical approval. Users can download relevant data freely for research and publication of relevant articles. This study is based on open-source data, so there are no ethical issues or other conflicts of interest. Based on the above criteria, patients were included in the training(n=113) and external validation(n=60) cohort.

Tumor delineation and radiomics features extraction

Employing 3D Slicer software (accessible at http://www.slicer.org), an experienced radiologist meticulously delineated lesions on venous phase CT images. This delineation process involved the creation of volumes of interest (VOI) on a per-slice basis. Subsequent to this meticulous delineation, Python's "pyradiomics" package was used to extract a total of 107 radiomics features from these VOIs, which can be categorized into three groups: 1) first-order features, 2) shape-based features, and 3) texture-based features.

Construction of radiomics signature

To assess the reproducibility of radiomics features, interclass correlation coefficients (ICC) were used. Twenty lesions were randomly selected and delineated by two radiologists. ICC values were computed for the radiomics features, and those meeting the criteria (ICC > 0.75) were retained. To prevent overfitting, we applied the least absolute shrinkage and selection operator logistic regression and 10-fold cross-validation to the training cohort using the selected radiomics features to construct the radiomics signature(Rad-score). These chosen features were weighted, summed, and combined with the intercept to generate the radiomics signature, referred to as the Rad-score.

Model assessment

The receiver operating characteristic curve (ROC) was generated for the Rad-score, and the corresponding area under the curve (AUC) was calculated to evaluate the Rad-score. The optimal cutoff point of the Rad-score was determined using the Youden index in the training cohort, and based on this point, the sensitivities, specificities, and accuracies of the Rad-score were computed. Calibration curves were employed to assess the calibration of the Rad-score, and the Hosmer-Lemeshow tests were performed to evaluate the goodness of fit.

Statistical analysis

The statistical analyses were conducted using R software (version 4.0.3), freely available on the official website of R Project (https://www.r-project.org/). Categorical variables were assessed using Chi-square or Fisher's exact test, while continuous

variables were examined using a t-test or Wilcoxon test. The "glmnet" package was utilized to perform LASSO logistic regression on the radiomics features. The "pROC" package was utilized for calculating the AUC and the Youden index. The "ggplot2" package was employed for generating ROC. The Hosmer-Lemeshow test was performed using the "generalhoslem" package. The "caret" package was employed for calculating ICC. P-value<0.05 was considered a statistically significant difference.

Results

Patient Characteristics

Table 1 displays the clinical factors of patients in both cohorts. There were no significant differences observed in age, Sex, Fuhrman grade, or TNM stage between the cohorts (P values between 0.115 and 0.736).

Construction of radiomics signature

Ninety-two features with ICC > 0.75 were retained. Subsequently, a LASSO logistic regression was conducted utilizing these features, which led to the selection of 8 radiomics features (**Figure 1**). The eight features and their corresponding coefficients are shown in **Table 2** :

In the training cohort, patients with high grade exhibited Rad-scores of 0.806 (0.301, 1.609), while those with low grade had Rad-scores of 0.110 (-0.0547, 0.496). In the validation cohort, the Rad-score ranges were 0.982 (0.696, 1.384) for high-grade patients and 0.483 (0.0132, 0.814) for low-grade patients. The Rad-scores of high-grade and low-grade patients exhibited significant differences in both cohorts(P<0.05). The boxplot diagram was plotted to visualize the distribution of the Rad-score.

Model assessment

The ROC curves of the Rad-score were generated **(Figure 3)**. The AUCs, accuracies, sensitivities, and specificities of the radiomics model in two cohorts are shown in **Table 3.** The calibration curves of the Rad-score in two cohorts were plotted **(Figure 4)**. As confirmed by Hosmer-Lemeshow testing, no significant differences existed between the actual and predicted probabilities in training (P=0.2177) and validation(P=0.0667) cohorts.

Discussion

In this study, we have developed a radiomics model for the purpose of predicting Fuhrman grade in patients diagnosed with ccRCC. Our radiomics model demonstrated remarkable predictive accuracy, achieving AUCs, accuracies, sensitivities, and specificities of 0.800, 78.76%, 86.49%, and 64.10% in the training cohort and 0.710, 71.67%, 97.22%, and 33.33% in the validation cohort. The radiomics model can potentially be a valuable tool for predicting Fuhrman grade in ccRCC patients, with promising levels of accuracy and calibration.

Many prior studies have explored the prediction of histological grades in various types of cancer using radiomics. For instance, one such study focused on pancreatic ductal adenocarcinoma, and their developed radiomics model achieved an AUC of 0.76 in the validation cohort[14]. Another study applied radiomics techniques based on preoperative magnetic resonance images to predict the histological grade of myxofibrosarcoma, where the radiomics model attained an impressive AUC value of 0.791 [15]. Furthermore, Hu et al. have focused on predicting the histopathologic grade of hepatocellular carcinoma (HCC) using radiomics based on preoperative Gadoxetic Acid-Enhanced MRI, resulting in a model with an AUC of 0.71[16]. Similarly, there have been studies using radiomics to predict histological grading in breast cancer[17], non-small cell lung cancer[18], and cervical cancer[19]. These studies collectively demonstrate the potential of radiomics in identifying histological grade in different cancer types. Radiomics can provide valuable insights and aid in non-invasive assessment and prediction of histological grade, which can inform treatment decisions and patient care.

Similar to these preceding studies, our research utilized preoperative CT images and radiomics to predict the Fuhrman grade of ccRCC. Eight radiomics features were selected to construct the Rad-score. Among these features, two are shape-related: original_shape_Maximum2DDiameterRow, which quantifies the largest pairwise Euclidean distance between tumor surface mesh vertices in the column-slice plane, and original_shape_Maximum2DDiameterSlice, which measures the largest pairwise Euclidean distance between tumor surface mesh vertices in the row-column plane. These two features are associated with the tumor's diameter. Previous research has suggested a correlation between larger tumor diameters and higher Fuhrman grade[20]. Consistent with this prior study, two radiomics features related to tumor diameter were selected in our research. Another selected radiomics feature is original_glcm_InverseVariance. Variance is a metric that measures heterogeneity, with higher values indicating a greater deviation in gray level values from their average. Therefore, a decreased original_glcm_InverseVariance suggests increased tumor

heterogeneity, which signifies a higher malignancy[21]. This may explain its negative correlation with the Fuhrman grade of ccRCC.The three features, original_glszm_GrayLevelNonUniformity, original_glszm_SizeZoneNonUniformity, and original_glszm_SizeZoneNonUniformityNormalized, are part of the Gray Level Size Zone Matrix features. They each provide insights into the tumor's heterogeneity.

original_glszm_GrayLevelNonUniformity measures the similarity of gray-level intensity values in the image. A lower GLNN value is indicative of greater similarity in intensity values. original_glszm_SizeZoneNonUniformity and original_glszm_SizeZoneNonUniformityNormalized assess the variability of size zone volumes throughout the image. A lower value suggests more uniformity among zone size volumes in the image. In all three radiomics features, higher values indicate increased tumor heterogeneity, which is associated with a higher malignancy. Additionally, there are two Neighbouring Gray Tone Difference Matrix Features: original_ngtdm_Coarseness, which measures the average difference between the center voxel and its neighborhood, providing insight into the spatial rate of change in intensity values and original_ngtdm_Contrast, a feature that quantifies the local intensity variation within the image. These features further contribute to the characterization of the tumor's heterogeneity. Based on the aforementioned selected eight radiomics features, the Rad-score was constructed. This approach yielded satisfactory accuracy in both the training(78.76%) and validation(71.67%) cohorts. This is higher in accuracy compared to the previously reported accuracy of 51.5% for Fuhrman grade was obtained through percutaneous needle core biopsy[22]. In two cohorts, patients with high grade exhibited significantly lower Rad-scores compared to patients with low grade. There was high consistency between the actual and predicted probabilities in the calibration curve of the radiomics model. This demonstrates that the Rad-score holds predictive value for the Fuhrman grade of RCC patients.

Our findings should be viewed in the context of certain limitations. Firstly, this study involved alimited number of patients, highlighting the necessity for a larger cohort and prospective investigations to confirm our results. Secondly, as radiomics involves high-dimensional data, there is a possibility of filtering out some meaningful features during the feature selection process. In the future, expanding the sample size is essential to ensure that important features are retained.

Conclusion

In conclusion, our study has developed a radiomics model for predicting the Fuhrman grade in patients with ccRCC. This model may serve as a non-invasive biomarker, offering a valuable tool for predicting Fuhrman grade in ccRCC patients.

References

[1] D'Avella C, Abbosh P, Pal SK and Geynisman DM. Mutations in renal cell carcinoma. Urol Oncol 2020; 38: 763-773.

[2] Xue W, Jian W, Meng Y, Wang T, Cai L, Yu Y, Yu Y, Xia Z and Zhang C. Knockdown of SETD2 promotes erastin-induced ferroptosis in ccRCC. Cell Death Dis 2023; 14: 539.

[3] Kloppel G, Knofel WT, Baisch H and Otto U. Prognosis of renal cell carcinoma related to nuclear grade, DNA content and Robson stage. Eur Urol 1986; 12: 426-431.

[4] Guethmundsson E, Hellborg H, Lundstam S, Erikson S, Ljungberg B and Swedish Kidney Cancer Quality Register G. Metastatic potential in renal cell carcinomas </=7 cm: Swedish Kidney Cancer Quality Register data. Eur Urol 2011; 60: 975-982.

[5] Delahunt B, Eble JN, Egevad L and Samaratunga H. Grading of renal cell carcinoma. Histopathology 2019; 74: 4-17.

[6] Blumenfeld AJ, Guru K, Fuchs GJ and Kim HL. Percutaneous biopsy of renal cell carcinoma underestimates nuclear grade. Urology 2010; 76: 610-613.

[7] Lebret T, Poulain JE, Molinie V, Herve JM, Denoux Y, Guth A, Scherrer A and Botto H. Percutaneous core biopsy for renal masses: indications, accuracy and results. J Urol 2007; 178: 1184-1188; discussion 1188.

[8] Patel HD, Johnson MH, Pierorazio PM, Sozio SM, Sharma R, Iyoha E, Bass EB and Allaf ME. Diagnostic Accuracy and Risks of Biopsy in the Diagnosis of a Renal Mass Suspicious for Localized Renal Cell Carcinoma: Systematic Review of the Literature. J Urol 2016; 195: 1340-1347.

[9] Gillies RJ, Kinahan PE and Hricak H. Radiomics: Images Are More than Pictures, They Are Data. Radiology 2016; 278: 563-577.

[10] Budai BK, Stollmayer R, Ronaszeki AD, Kormendy B, Zsombor Z, Palotas L, Fejer B, Szendroi A, Szekely E, Maurovich-Horvat P and Kaposi PN. Radiomics analysis of contrast-enhanced CT scans can distinguish between clear cell and non-clear cell renal cell carcinoma in different imaging protocols. Front Med (Lausanne) 2022; 9: 974485.

[11] Deniffel D, McAlpine K, Harder FN, Jain R, Lawson KA, Healy GM, Hui S, Zhang X, Salinas-Miranda E, van der Kwast T, Finelli A and Haider MA. Predicting the recurrence risk of renal cell carcinoma after nephrectomy: potential role of CT-radiomics for adjuvant treatment decisions. Eur Radiol 2023; 33: 5840-5850.

[12] Rossi E, Boldrini L, Maratta MG, Gatta R, Votta C, Tortora G and Schinzari G. Radiomics to predict immunotherapy efficacy in advanced renal cell carcinoma: A retrospective study. Hum Vaccin Immunother 2023; 19: 2172926.

[13] Clark K, Vendt B, Smith K, Freymann J, Kirby J, Koppel P, Moore S, Phillips S, Maffitt D, Pringle M, Tarbox L and Prior F. The Cancer Imaging Archive (TCIA): maintaining and operating a public information repository. J Digit Imaging 2013; 26: 1045-1057.

[14] Cen C, Wang C, Wang S, Wen K, Liu L, Li X, Wu L, Huang M, Ma L, Liu H, Wu H and Han P. Clinical-radiomics nomogram using contrast-enhanced CT to predict histological grade and survival in pancreatic ductal adenocarcinoma. Front Oncol 2023; 13: 1218128.

[15] Yao Y, Zhao Y, Lu L, Zhao Y, Lin X, Xia J, Zheng X, Shen Y, Cai Z, Li Y, Yang Z and Lin D. Prediction of histopathologic grades of myxofibrosarcoma with radiomics based on magnetic resonance imaging. J Cancer Res Clin Oncol 2023; 149: 10169-10179.

[16] Hu X, Li C, Wang Q, Wu X, Chen Z, Xia F, Cai P, Zhang L, Fan Y and Ma K. Development and External Validation of a Radiomics Model Derived from Preoperative Gadoxetic Acid-Enhanced MRI for Predicting Histopathologic Grade of Hepatocellular Carcinoma. Diagnostics (Basel) 2023; 13:

[17] Wang S, Wei Y, Li Z, Xu J and Zhou Y. Development and Validation of an MRI Radiomics-Based Signature to Predict Histological Grade in Patients with Invasive Breast Cancer. Breast Cancer (Dove Med Press) 2022; 14: 335-342.

[18] Tang X, Bai G, Wang H, Guo F and Yin H. Elaboration of Multiparametric MRI-Based Radiomics Signature for the Preoperative Quantitative Identification of the Histological Grade in Patients With Non-Small-Cell Lung Cancer. J Magn Reson Imaging 2022; 56: 579-589.

[19] Liu Y, Zhang Y, Cheng R, Liu S, Qu F, Yin X, Wang Q, Xiao B and Ye Z. Radiomics analysis of apparent diffusion coefficient in cervical cancer: A preliminary study on histological grade evaluation. J Magn Reson Imaging 2019; 49: 280-290.

[20] Zhang C, Li X, Hao H, Yu W, He Z and Zhou L. The correlation between size of renal cell carcinoma and its histopathological characteristics: a single center study of 1867 renal cell carcinoma cases. BJU Int 2012; 110: E481-485.

[21] Faggioni L, Gabelloni M, De Vietro F, Frey J, Mendola V, Cavallero D, Borgheresi R, Tumminello L, Shortrede J, Morganti R, Seccia V, Coppola F, Cioni D and Neri E. Usefulness of MRI-based radiomic features for distinguishing Warthin tumor from pleomorphic adenoma: performance assessment using T2-weighted and post-contrast T1-weighted MR images. Eur J Radiol Open 2022; 9: 100429.

[22] Sofikerim M, Tatlisen A, Canoz O, Tokat F, Demirtas A and Mavili E. What is the role of percutaneous needle core biopsy in diagnosis of renal masses? Urology 2010; 76: 614-618.

Table 1 Clinical factors in two cohorts

Clinical factors	**Training cohort (n=113)**	**validation cohort (n=60)**	**P-value**
Age	59.60±11.46	62.65±13.06	0.115
laterality			0.385
Left	53	24	
right	60	36	
Sex			0.342
male	76	36	
female	37	24	
Grade			0.475
G1/G2	39	24	
G3/G4	74	36	
TNM stage			0.736
I	59	31	
II	8	4	
III	29	19	
IV	17	6	

Table 2 selected radiomics features and their corresponding coefficients

Radiomics features	Coefficients
(Intercept)	0.617373717
original_shape_Maximum2DDiameterRow	0.015140683
original_shape_Maximum2DDiameterSlice	0.00393793
original_glcm_InverseVariance	-4.11088489
original_glszm_GrayLevelNonUniformityNormalized	4.658666714
original_glszm_SizeZoneNonUniformity	1.02E-05
original_glszm_SizeZoneNonUniformityNormalized	2.431619523
original_ngtdm_Coarseness	-64.66623256
original_ngtdm_Contrast	-17.72034724

Table 3 Model performance in two cohorts

	Training cohort (n=113)				Test cohort (n=60)			
Model	AUC	Accuracy	Sensitivity	Specificity	AUC	Accuracy	Sensitivity	Specificity
Radiomics model	0.800	78.7610%	86.48649%	64.10256%	0.710	71.66666%	97.22222%	33.33333 %

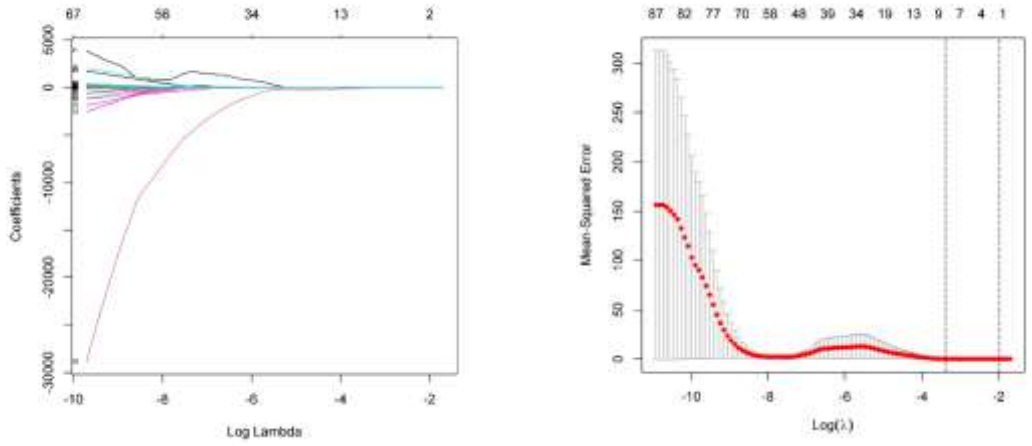

(**a**) (**b**)

Figure 1 Radiomics feature selection(a) LASSO coefficient profiles. (b) 10-fold cross-validation. The optimal lambda value: Log (Lambda) =-3.381(corresponding to Lambda = 0.034), was chosen using 10-fold cross-validation.

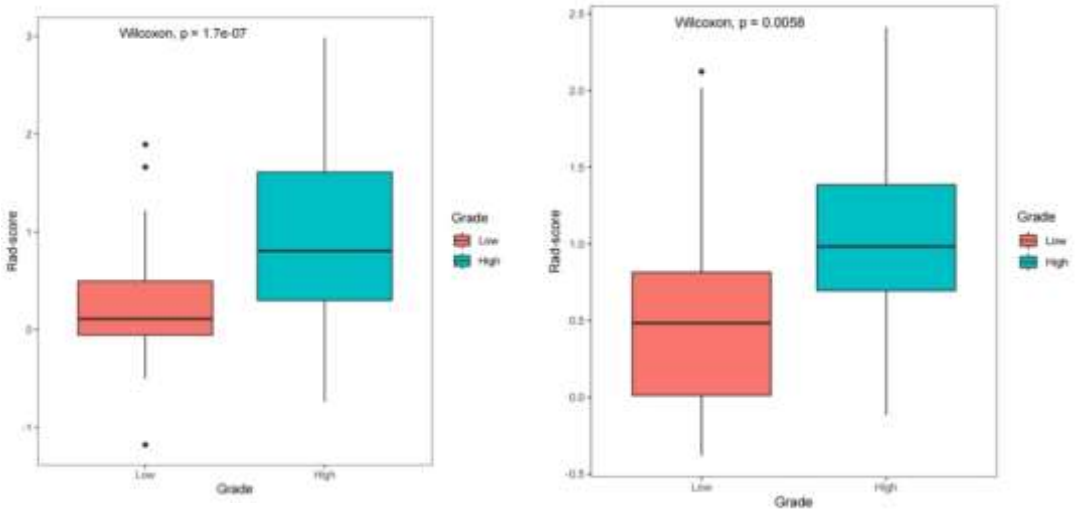

(**a**) (**b**)

Figure 2 Distribution of Rad-score in training(a) and validation(b) cohorts visualized by a boxplot diagram

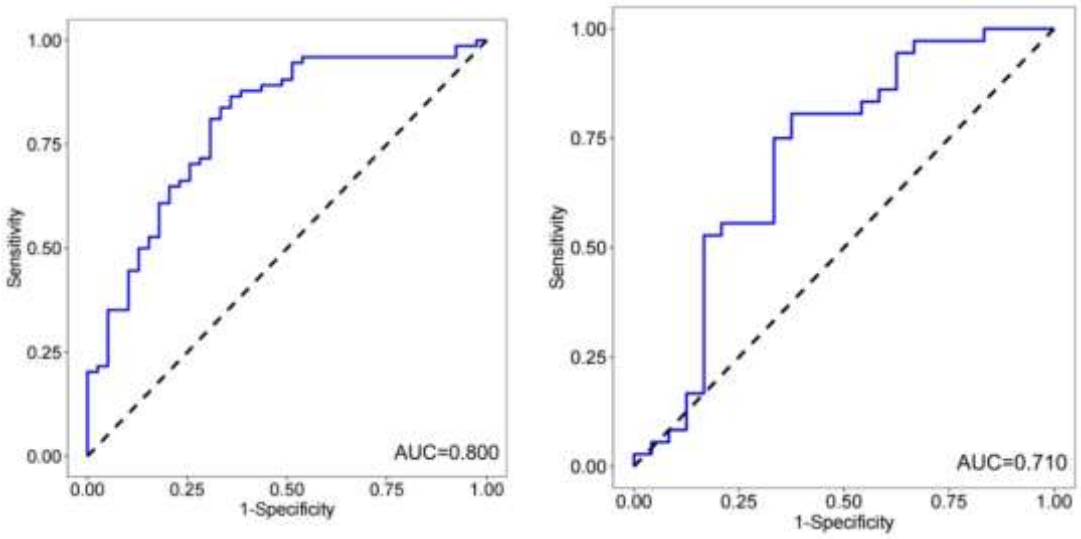

(**a**) (**b**)

Figure 3 The ROC of the radiomics model in the (a) training and (b) validation cohorts.

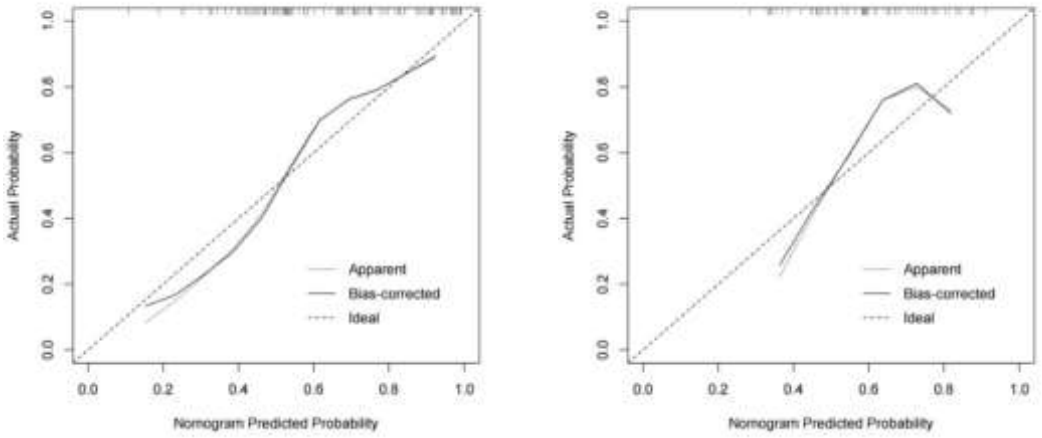

(**a**) (**b**)

Figure 4 Calibration curves of the radiomics model for the (a) training and (b) validation cohorts.